LASER VELOCIMETER APPLICATIONS TO HIGH-LIFT RESEARCH

R. R. Whipkey, G. Jones, and J. A. Braden
Lockheed-Georgia Co.
Marietta, Georgia

The subject of this presentation concerns the application of the Lockheed-Georgia 2-D laser velocimeter (LV) burst-counter system to the flow field around a 2- and 3-element high-lift airfoil. This work, performed under contract to NASA Langley Research Center, evaluates, via the LV, the characteristic behavior of the confluent boundary layer (that is, the boundary layer existing downstream of a slot) as it approaches and undergoes separation. In this application, the LV represents all ideal instruments for nonintrusively probing into the narrow slots and cove areas characterizing mechanical high-lift systems. The work is being performed in the Lockheed-Georgia 10 × 30-inch low-speed test facility using a 9-inch (basic) chord section of the general aviation GAW-1 airfoil. Figure 1 shows the test facility and LV-system arrangements used in the experimental work. The LV system (ref. 1) employs a 4-W argon laser and operates in an off-axis, backscatter mode with a focal length of about 30 inches. Smoke is used as the seeding medium and is injected downstream of the model such that particle uniformity and size are constant upon completion of the tunnel circuit into the test area. The LV system (fig. 1) is fully automated by utilizing a MAC-16 minicomputer for positioning, data acquisition, and preliminary data reduction.

Figure 2 summarizes the matrix of airfoil configurations undergoing current study where the behavior of the boundary layer reflects modifications in the slots and angular deflections of the leading- and trailing-edge airfoil elements. With this rather extensive matrix of study configurations it has become expedient to use various devices by which nominal flow surveys can be rapidly acquired and those areas of specific interest (separated flow, vortex formations, and so forth) can be quickly identified for more precise measurements. A highly reliable method for this purpose is represented by a "quick-traverse" LV-analog system which is employed to acquire instantaneous velocity profiles. This is normally done prior to obtaining the more time-consuming digital definition of the boundary layers in terms of mean velocity profiles u and v, Reynolds shear stresses, and turbulence intensities u' and v'. Figure 3 shows a sample output from the analog system as compared to the corresponding digital data (bottom of the figure) for an attached- and separated-flow condition on the airfoil. As noted, the quick-traverse analog trace provides a reliable indication of the position and degree of surface-flow separation as well as the shape and condition of the overall boundary-layer profile.

The extent of LV data acquisition for boundary layers on the individual airfoil configurations is exemplified in figure 4, which shows the airfoil at a post-stall angle of attack of 16°. The corresponding pressure distribution, also shown on figure 4, indicates a trailing-edge type of flow separation on the main airfoil element which is further corroborated by the boundary-layer surveys. Points of general interest in such surveys are the large wake overlying the flap-surface flow, the stationary vortex within the cove area, and the modifications to the main-element, upper-surface flow as introduced by variations in the leading-edge geometry. For most trailing-edge configurations, it has been found that attached flap-surface flow is maintained for all but the most adverse circumstances although the flap load (i.e., lift) is highly sensitive to the separated wake from the forward main element. Corresponding to the velocity profiles displayed in figure 4, the turbulence intensity and Reynolds shearing stress profiles are presented in figures 5 to 7. Figures 5 and 6 show the streamwise and normal (to the airfoil surface) components of the turbulence-intensity measurements representing coincident data points as acquired by the LV system. These data and the shearing stress data of figure 7 show the high level of turbulence within the separated wake and the shear layer near its edges.

To further enhance the visual interpretation of general flow behavior, computer graphics are extensively employed to treat specific areas of the flow field as illustrated in figures 8 to 10. In these figures, the leading-edge, trailing-edge, and wake flow fields are highlighted by enlargement. In many instances of massive flow separation the measured time-averaged velocity profiles will reflect the highly unsteady nature of the flow through slight variations in the magnitude of adjacent velocity vectors and, in isolated instances, through variations in flow direction (wakes primarily). In the leading-edge regions (fig. 8), characterized by high-speed, curvilinear flows, close-to-surface LV measurements become difficult as (it is speculated) the seeding medium tends to be "centrifuged" away from the surface. The generation of seeding particles of specified sizes and distributions using various media represents a current emphasis in further LV-development work at Lockheed, and additional research is needed to fully understand these effects.

Further effective use of computer graphics for interpreting the measured flow fields is illustrated in figure 11, wherein contours of constant velocity components (u) are shown. Such charts, developed for rapid visualization of all LV measurements, facilitate data manipulations as needed for interfacing with theoretical modeling of the flow field. The rapidity and consistency of the LV system for acquiring such data makes it mandatory that an extensive data processing capability be an inherent part of the experimental setup.

RIREFERENCE

1. Whiffen, M. C.; and Meadows, D. M.: Two Axis Single Particle Laser Velocimeter System for Turbulence Spectral Analysis. Proc. of the Second International Workshop on Laser Velocimetry, Vol. 1, Mar. 1974, pp. 1-12.

Figure 1.- Experimental arrangement of 2-D LV system in the 10 × 30-inch low-speed test facility.
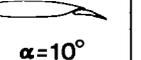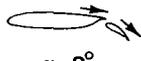
CLEAN AIRFOIL	$\alpha=0°$	$\alpha=4°$	$\alpha=8°$	$\alpha=10°$	$\alpha=12°$	$\alpha=16°$
FLAPPED $\delta_f=20°$	$\alpha=8°$	$\alpha=12°$	$\alpha=16°$	$\alpha=8°$	$\alpha=12°$	$\alpha=16°$
FLAPPED $\delta_f=30°$	$\alpha=4°$	$\alpha=8°$	$\alpha=12°$	$\alpha=4°$	$\alpha=8°$	$\alpha=12°$
FLAPPED $\delta_f=40°$	$\alpha=4°$	$\alpha=8°$	$\alpha=10°$	$\alpha=4°$	$\alpha=8°$	$\alpha=11°$
SLATTED $\delta_s=45°$						
FLAPPED & SLATTED $\delta_f=30°$ $\delta_s=45°$	$\alpha=12°$	$\alpha=14°$	$\alpha=16°$	$\alpha=12°$	$\alpha=14°$	$\alpha=16°$
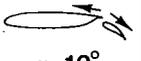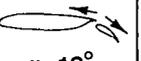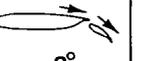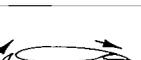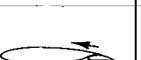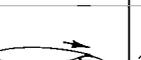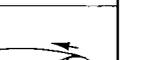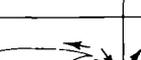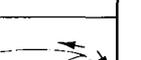
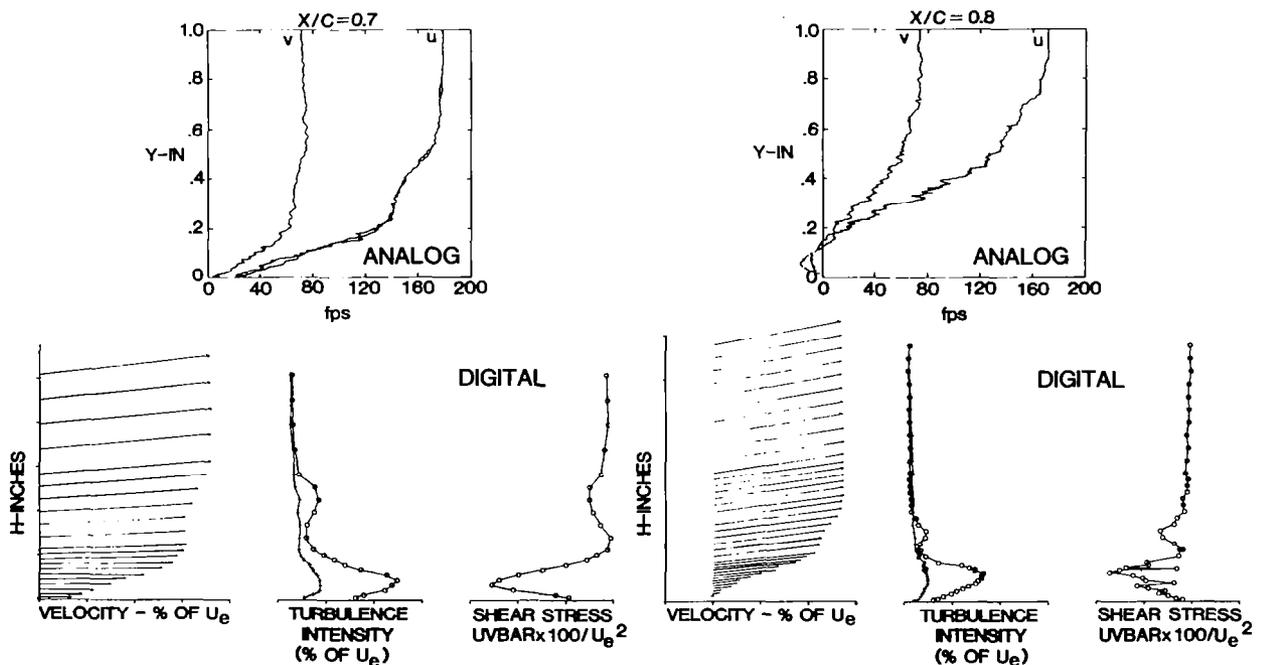Figure 2.- Applications to high-lift research - separating confluent boundary layer.

Figure 3.- Analog rapid-scan LV system. GAW-1 airfoil; $\delta_f = 30°$; $\alpha = 16°$.
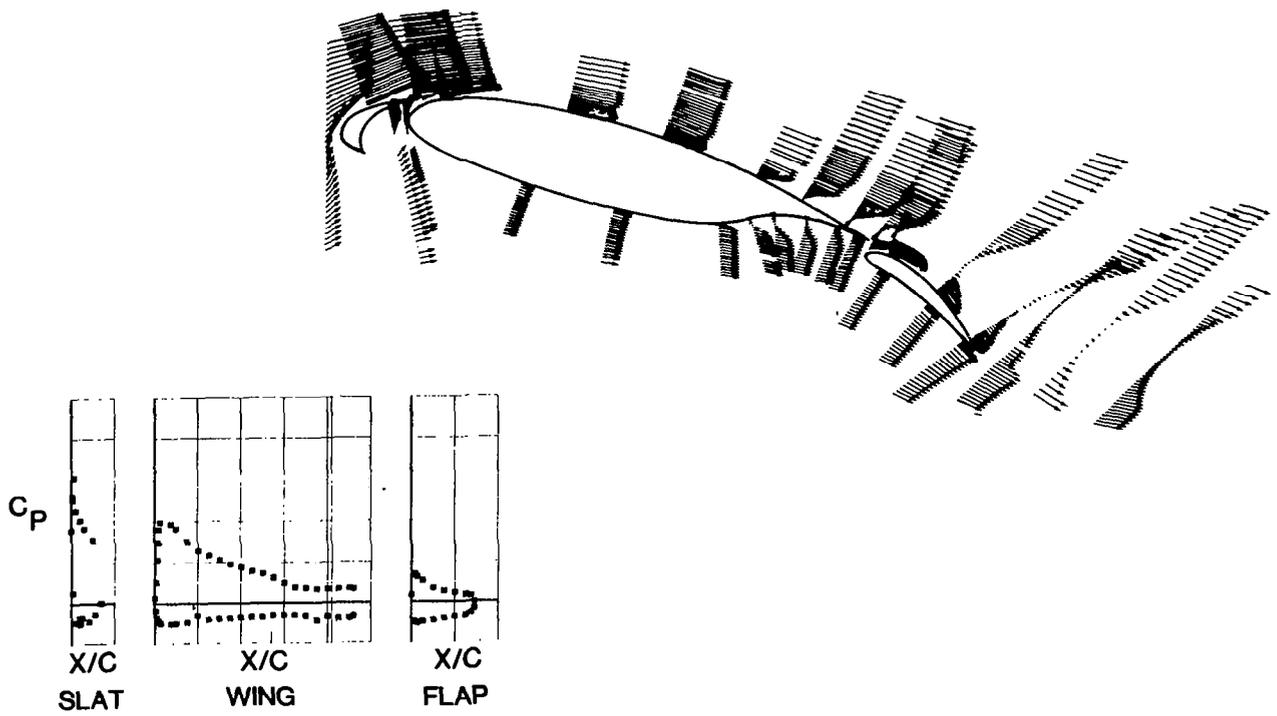
Figure 4.- Example of LV data acquisition for GAW-1 airfoil velocity vectors. $\alpha = 16^{\circ}$.
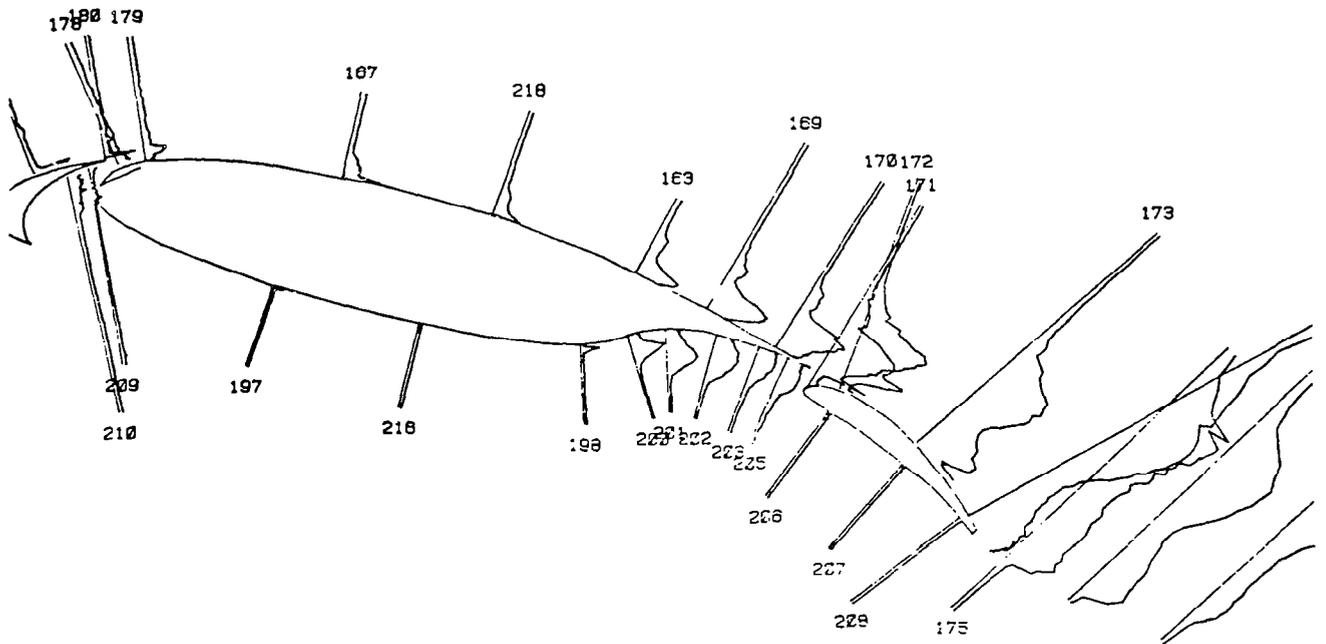

Figure 5.- Streamwise component of turbulence intensity u'. GAW-1 airfoil; $\delta_f = 30^{\circ}$; $\alpha = 16^{\circ}$.

278
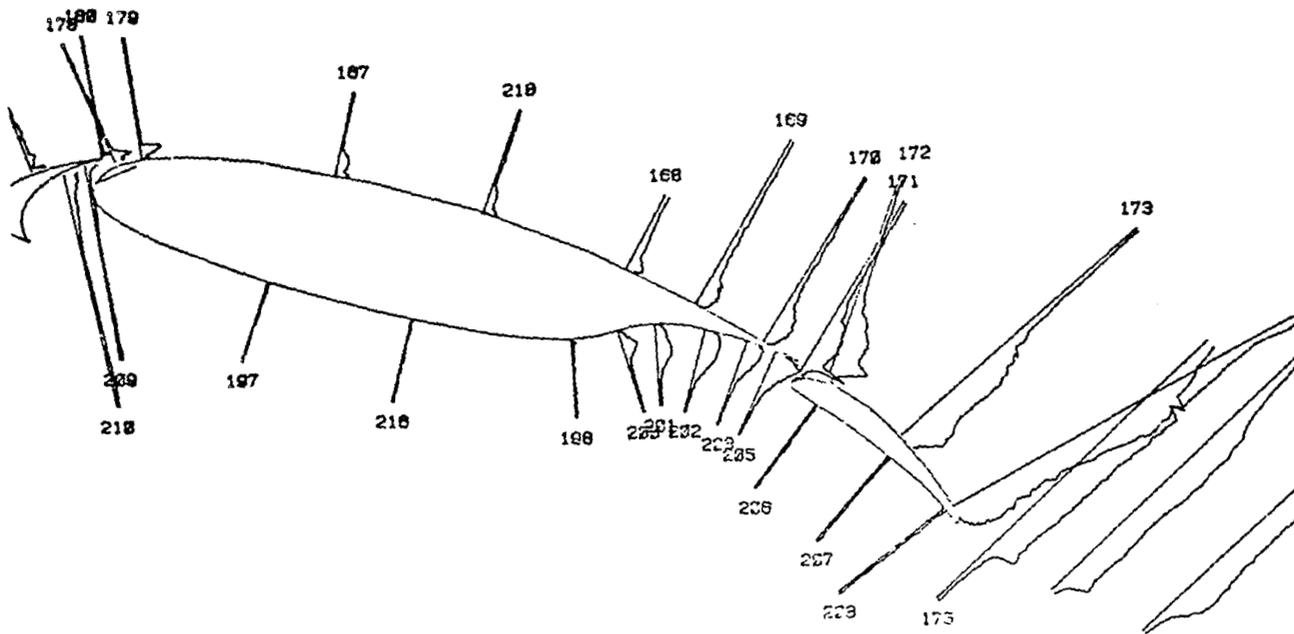
Figure 6.- Normal component of turbulence intensity v'. GAW-1
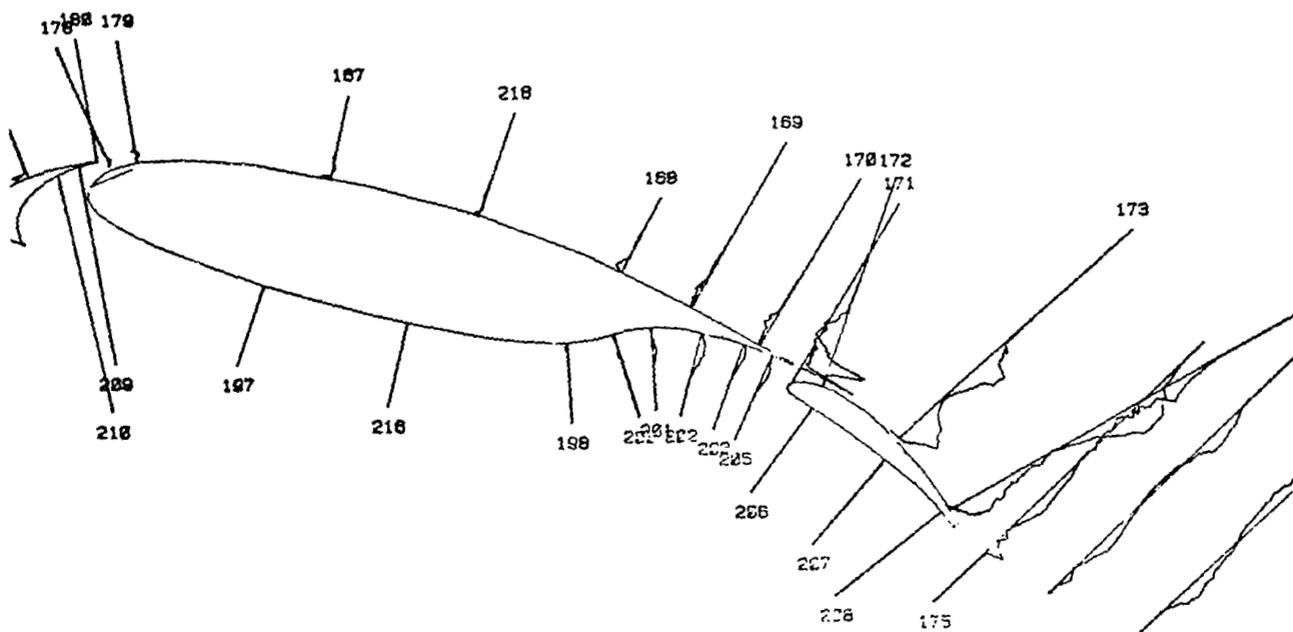airfoil; $\delta_f = 30^o$; $\alpha = 16^o$.

Figure 7.- Reynolds shearing stress profiles u'v'. GAW-1 airfoil;
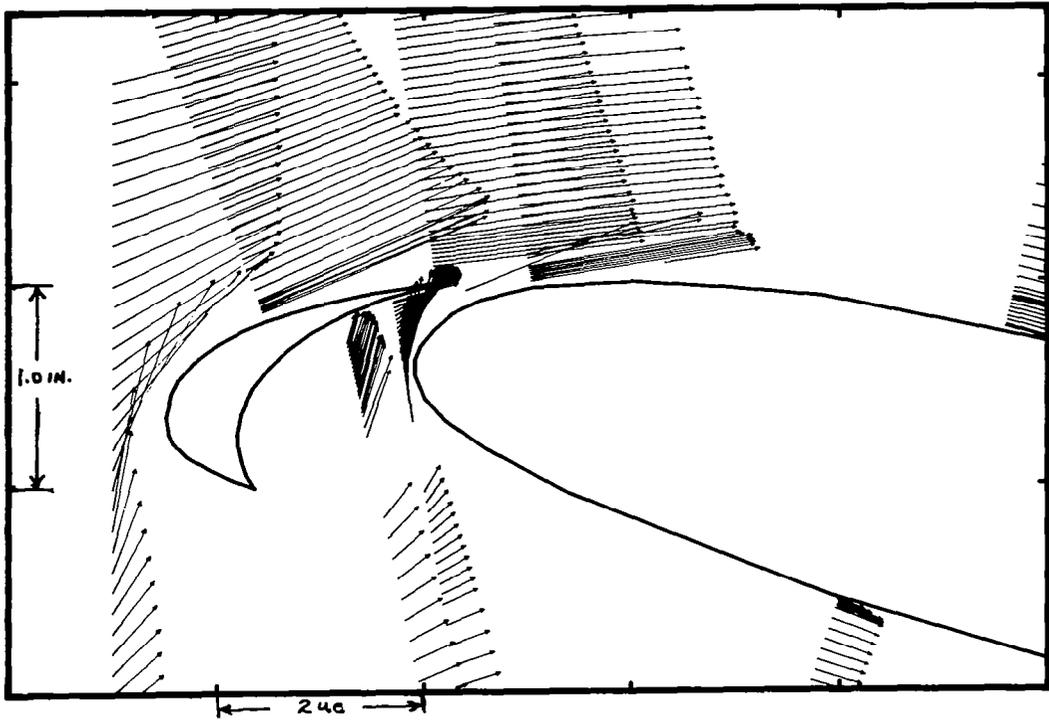$\delta_f = 30^o$; $\alpha = 16^o$.

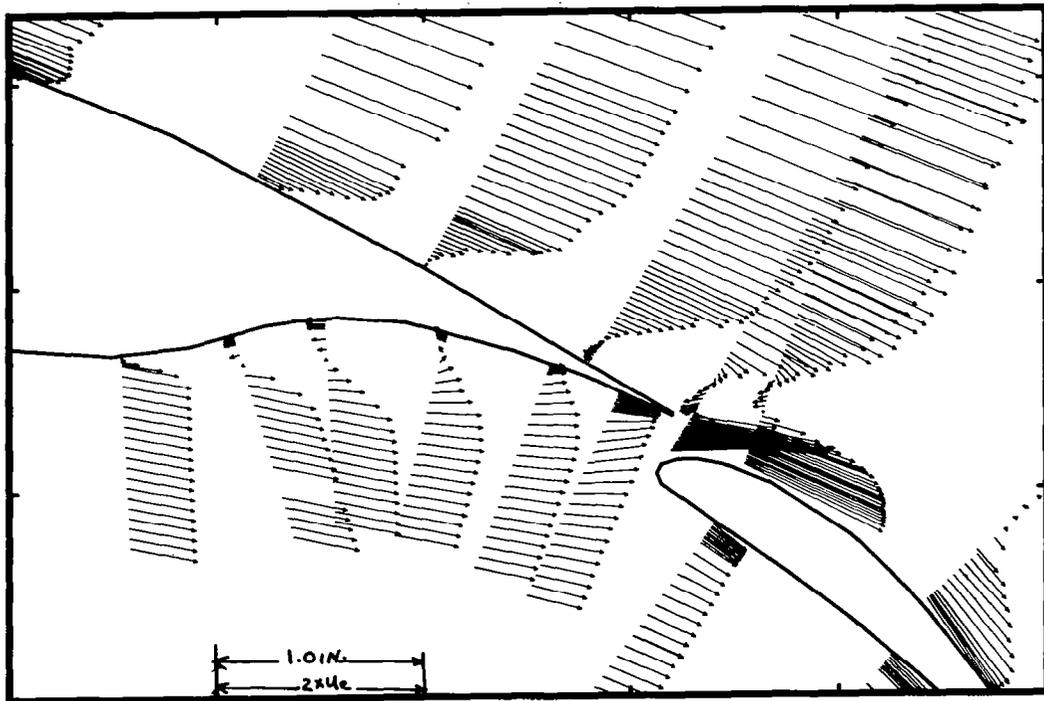Figure 8.- Leading-edge flow field. GAW-1 airfoil; $\delta_f = 30^o$; $\alpha = 16^o$.

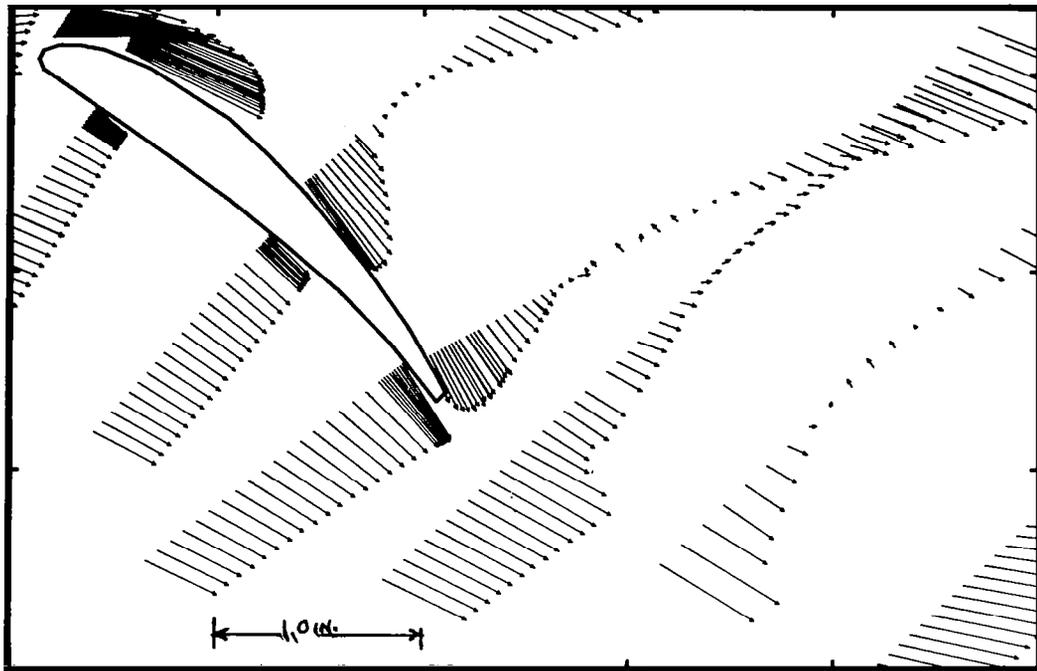Figure 9.- Trailing-edge flow field. GAW-1 airfoil; $\delta_f = 30^o$; $\alpha = 16^o$.

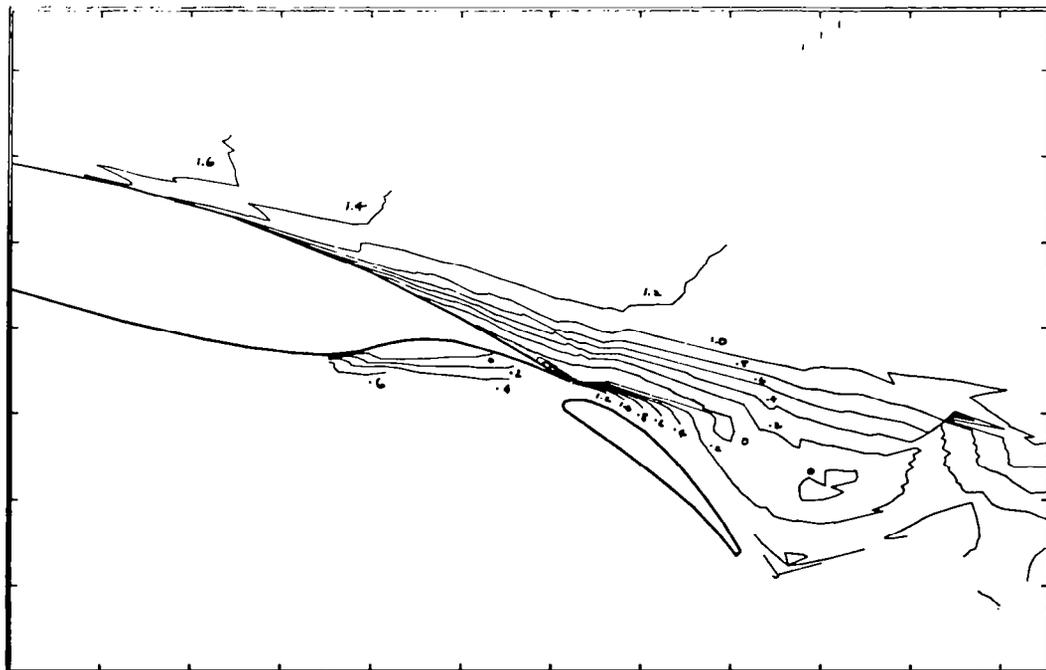Figure 10.- Wake flow field. GAW-1 airfoil; $\delta_f = 30^o$; $\alpha = 16^o$.

Figure 11.- Contours of constant velocity components u. GAW-1 airfoil; $\delta_f = 30^o$; $\alpha = 16^o$.